APL Materials

High hole mobility and non-localized states in amorphous germanium

Tuan T. Tran ✉ 🆔 ; Jennifer Wong-Leung; Lachlan A. Smillie; Anders Hallén 🆔 ; Maria G. Grimaldi;
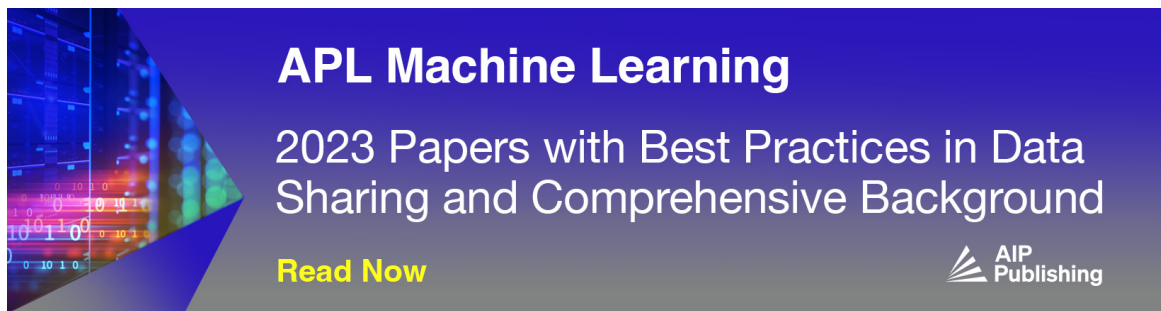Jim S. Williams

Check for updates

CrossMark

View
Online

Export
Citation

20 March 2024 08:52:23

AIP Publishing

High hole mobility and non-localized states in amorphous germanium

View Online　　Export Citation　　CrossMark

Tuan T. Tran,[1,2,a] (ID) Jennifer Wong-Leung,[2] Lachlan A. Smillie,[2] Anders Hallén,[3] (ID) Maria G. Grimaldi,[4] and Jim S. Williams[2]

AFFILIATIONS

[1] Department of Physics and Astronomy, Uppsala University, Lägerhyddsvägen 1, S-75237 Uppsala, Sweden
[2] Department of Electronic Materials Engineering, Research School of Physics and Engineering, Australian National University, Canberra, ACT 0200, Australia
[3] KTH—Royal Institute of Technology, School of Information and Communication Technology, PO Box 229, SE-164 40 Kista, Sweden
[4] CNR-IMM MATIS and Department of Physics and Astronomy, University of Catania, Via S. Sofia 64, I-95123 Catania, Italy

[a] Author to whom correspondence should be addressed: Tuan.Tran@physics.uu.se

ABSTRACT

Covalent amorphous semiconductors, such as amorphous silicon (a-Si) and germanium (a-Ge), are commonly believed to have localized electronic states at the top of the valence band and the bottom of the conduction band. Electrical conductivity is thought to occur through the hopping mechanism via these localized states. The carrier mobility of these materials is usually very low, in the order of $\sim 10^{-3}$–10^{-2} cm^2/Vs at room temperature. In this study, we show that pure high-density amorphous Ge has exceptionally high carrier mobility, in the order of ~ 100 cm^2/Vs, and a high hole concentration of $\sim 10^{18}$ cm^{-3}. The temperature-dependent conductivity of the material is also very-well defined with two distinctive regions, extrinsic and intrinsic conductivity, as in crystalline Ge. These results provide direct evidence for a largely preserved band structure and non-localized states within the valence band in high-density amorphous Ge, as previously suggested by Tauc *et al.* from optical characterization alone.

INTRODUCTION

Amorphous semiconductors are an important set of materials, with a wide range of applications, such as thin film solar cells, flat panel displays, thin film electronics, and wearable devices.[1] The unique advantages of amorphous semiconductors include the possibility of producing the materials by low-cost deposition techniques on many types of substrates (including flexible substrates) with a low thermal budget, even at room temperature. Due to the lack of translational symmetry, theoretical calculations of the electronic band structure of amorphous materials are difficult.[2] Nevertheless, a simplified one-dimensional case has been solved, providing some important features of these disordered materials.[3] Treating the amorphous phase as a perturbation from the periodic structure, Gubanov has shown that a bandgap exists in disordered phases but the electronic wave functions become localized at the band extrema.

Depending on the degree of disorder, the localized states can extend from the band extrema into the bandgap and form the band tail. The localized states can also form within the bandgap, around the Fermi level as shown in Fig. 1. In this localized band, electrons cannot travel at zero temperature. At higher temperatures, an electron can travel by jumping from site to site thanks to thermal excitation, thus called hopping conduction.[4] In crystalline semiconductors, the conduction occurs mostly at the band extrema. The border between the bandgap and the conducting bands is well-defined, leading to a well-defined conductivity with temperature. In the amorphous phase, the conductivity can occur over a wider range of localized bands with a "fuzzy" band structure, leading to a less-defined behavior of the conductivity.

It is challenging to reconcile all the available experimental data and to construct a unified band structure for amorphous materials because their properties are particularly dependent on the
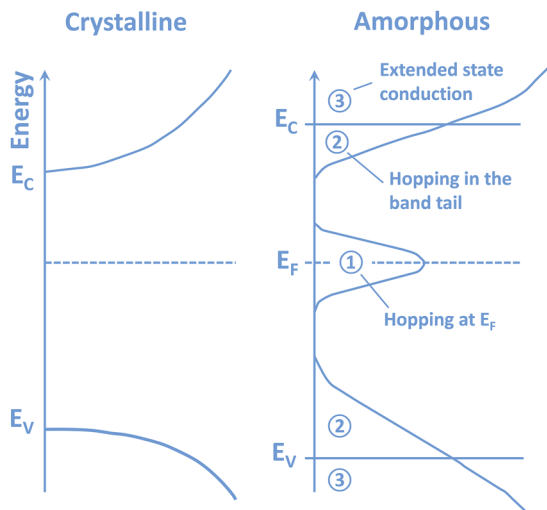
FIG. 1. Schematic band structure of crystalline (left) and amorphous semiconductors (right). Included are the different types of conductivity in the amorphous phase. Figure adapted from Ref. 5.

experimental parameters, such as the fabrication processes and sample history, which affect the mass density and the purity of the materials. It is reported that the conductivity and the thermoelectric power of amorphous germanium (a-Ge) and silicon (a-Si) prepared by electron-beam evaporation vary quite markedly with the substrate temperature during deposition, evaporation rate, and the ambient pressure.[6] Aging effects and the absorption of impurities from the ambient can also change the electrical conductivity, with significant film to film variability.[7] For example, reports on the conductivity type of a-Ge are conflicting as to whether it is intrinsically p-type or n-type. Using Hall effect measurements, Clark reported that the conductivity is n-type with a carrier concentration of the order of 10^{18} cm^{-3},[8] whereas Tauc's co-workers indicated that a-Ge has p-type conductivity with a carrier concentration of $\sim 10^{17}$–10^{18} cm^{-3}, regardless of the dopant in the evaporated materials.[9,10] Most of the electrical characterization results to date seem to agree that the carrier mobility of deposited a-Ge is less than $\sim 10^{-2}$ cm^2/(Vs), presumably leading to a conclusion that the electronic wave function is localized, and the conductivity is by the hopping mechanism.

In contrast to electrical characterization, optical characterization studies support non-localized states in a-Ge.[2] Studying the absorption spectra of a-Ge from 0.08 to 1.6 eV, Tauc *et al.* could observe the optical transition characteristics of the three branches of the valence band.[10] These transitions are well-described by a set of formulas used for crystalline Ge (c-Ge). Calculation of the hole effective mass and the spin–orbit splitting energy also showed comparable values to crystalline Ge. The conclusions of this study were that the valence band of the a-Ge is not much different from that of c-Ge and the wave-function of the valence band is non-localized as in c-Ge.[9–11] However, such an extended wave function in a-Ge has not been well accepted in the literature because the carrier mobility, as measured by electrical conductivity, is reported to be

4 orders of magnitude lower than what it should be if the wave function was non-localized. It is noteworthy that all the a-Ge samples in the literature have been prepared by deposition techniques in which the material density varies largely from 72% to 95% of the c-Ge value.[8,12,13] This reduced density, as well as impurity content, might cause fluctuations in mass distribution in the films, which might affect the electrical conductivity.

In order to minimize the contributions of mass-density fluctuations and impurities, in this study, we prepared a pure a-Ge layer using an ion-beam amorphization process of a crystalline Ge layer.[14,15] The prepared material is completely disordered (amorphized) by an energetic beam of Ge$^+$ ions and, as such, is expected to exhibit a mass-density very close (>98.5%) to the value of crystalline Ge, as previously observed.[16]

Experiments

The starting samples consist of ~ 0.92 μm of undoped c-Ge grown by chemical vapor deposition on Si(100) substrates. The amorphization process was done by implanting ^{74}Ge$^+$ ions into the substrate at an energy of 2.5 MeV and a dose of 110^{15} cm^{-2}. The samples were rotated 7° off the normal axis to avoid channeling and also kept at liquid nitrogen temperature to avoid ion-beam induced porosity.[17,18] According to a SRIM simulation,[19] these implant parameters are able to induce complete disordering of the original Ge crystal, with the calculated displacement-per-atom (*dpa*) >2 over the Ge layer. The amorphous layer is, furthermore, predicted to extend ~ 1.1 μm into the Si substrate. A previous study has shown that a *dpa* value of ~ 0.3 is sufficient for the complete amorphization of a Ge crystal.[14] The purpose of using such a sample structure is to utilize the insulating property of a-Si, which has a resistivity in the order of 10^5 Ω cm,[20] in order to measure electrical transport only in the a-Ge layer. It will be shown later that the resistivity ratio ρ_{a-Si}/ρ_{a-Ge} is at least 6 orders of magnitude. Therefore, the a-Si layer effectively isolates the a-Ge layer from the substrate for the purposes of electrical characterization. In the Supplementary section, we provide more details on the SRIM simulation and results. To verify the amorphization of the samples, we employed cross-sectional transmission electron microscopy (XTEM) and selective area electron diffraction (SAED) on samples prepared by focused ion beam (FIB).

Electrical characterization was carried out using a Lakeshore 7707 temperature-dependent Hall effect measurement system. The temperature range of the measurement was from 30 to 360 K using two different measurement stages: a closed cycle refrigerator stage for the temperature range of 30–290 K and a high temperature oven stage for the temperature range of 300–360 K. A 1×1 cm^2 van der Pauw sample structure was used where electrical contacts to the samples were provided by indium (In) solder bumps. The diameter of the In bumps was kept as small as possible and close to the 4 corners of the samples to minimize measurement errors related to the Van der Pauw structure. I–V measurement of the samples showed good Ohmic behavior of the contacts.

RESULTS AND DISCUSSION

Figures 2(a)–2(c) are the XTEM images showing the three distinct regions of the samples: the 0.92 μm Ge layer, the 1.1 μm
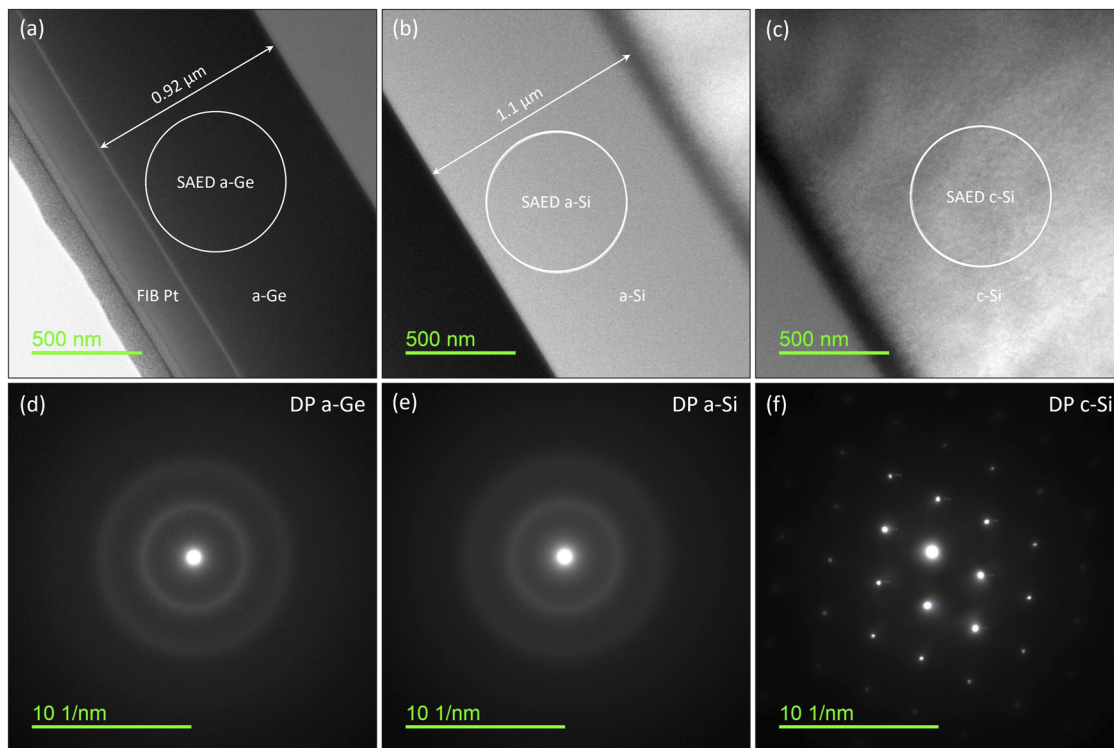
FIG. 2. Cross-sectional transmission electron micrographs of the Ge-on-Si substrate after implanted with 2.5 MeV ^{74}Ge$^+$ ions at a dose of 110^{15} cm^{-2}. (a)–(c) The cross sections of the three regions of the samples: the 0.92 μm a-Ge layer, the 1.1 μm a-Si layer, and the c-Si substrate. (d)–(f) The SAED patterns of the respective layers.

Si layer, and the undamaged c-Si substrate. The top layer is platinum deposited in the FIB chamber before the ion milling to protect the region-of-interest from the FIB process, particularly ion-beam damage. Both a-Ge and a-Si layers can be seen to be homogeneous and free of voids. The SAED patterns of the respective layers are shown in Figs. 2(d)–2(f). Particularly for the a-Ge and the a-Si layers, these diffraction patterns show uniform diffusing rings, without any evidence of diffraction spots and sharp streaks. The SAED patterns were also collected at different depths within the a-Ge layer, and each showed a similar diffuse pattern as in Fig. 2(d). This diffraction characterization indicates that the Ge and the Si layers after ion implantation have completely lost long-range order and have become fully amorphous.

Using the SAED data in Fig. 2, we deduced the radial distribution function (RDF) g(r) of the ion-implanted Ge. The calculation process of g(r) is described elsewhere in Ref. 21. The resulting RDF is shown in Fig. 3 (black solid curve), together with results from other studies (dash curves).[9,22–25] Since the RDF represents an average number of the Ge atoms as a function of the radial distance r from a reference atom, the function shows the atomic arrangement in solid and liquid materials. The RDF of crystalline materials is composed of extremely sharp peaks at certain distances from the center. For crystalline Ge, the distances of the 1st, 2nd, and 3rd coordinations are 2.43, 3.97, and 4.66 Å, respectively.[26] For amorphous Ge, the distribution of the 1st coordination broadens as shown by the first peak around 2.43 Å in Fig. 3. The distributions of the 2nd and the

3rd peaks are even wider, showing the fact that highly disordered or amorphous materials, to some extent, have short-range order. The nearest neighbor distance is still like the crystalline case, but this order quickly diminishes as the distance increases from the reference
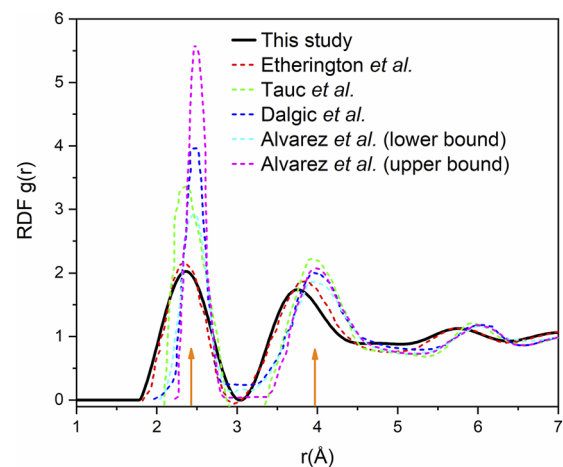
FIG. 3. Radial distribution function (RDF) of the implanted amorphous Ge as deduced from the electron diffraction data (solid black). Referenced results from other studies of amorphous Ge are also included.[9,22–25]

point. In comparison to the RDF of other studies, our distribution has a comparable integrated area below the peaks, such as ±7% for the first coordination. However, the peaks of our films appear to be shorter and broader, indicating that the degree of disorder in our films is higher than most films that are considered amorphous in literature.

In Fig. 4, the resistivity ρ and the Hall coefficient R_H obtained from the measurements are presented. In Fig. 4(a), our measured resistivity for the crystalline Ge substrate (blue-triangles) has a similar behavior to that reported by Putley.[27] This curve has two distinct regions with different slopes. The low-slope region in the low
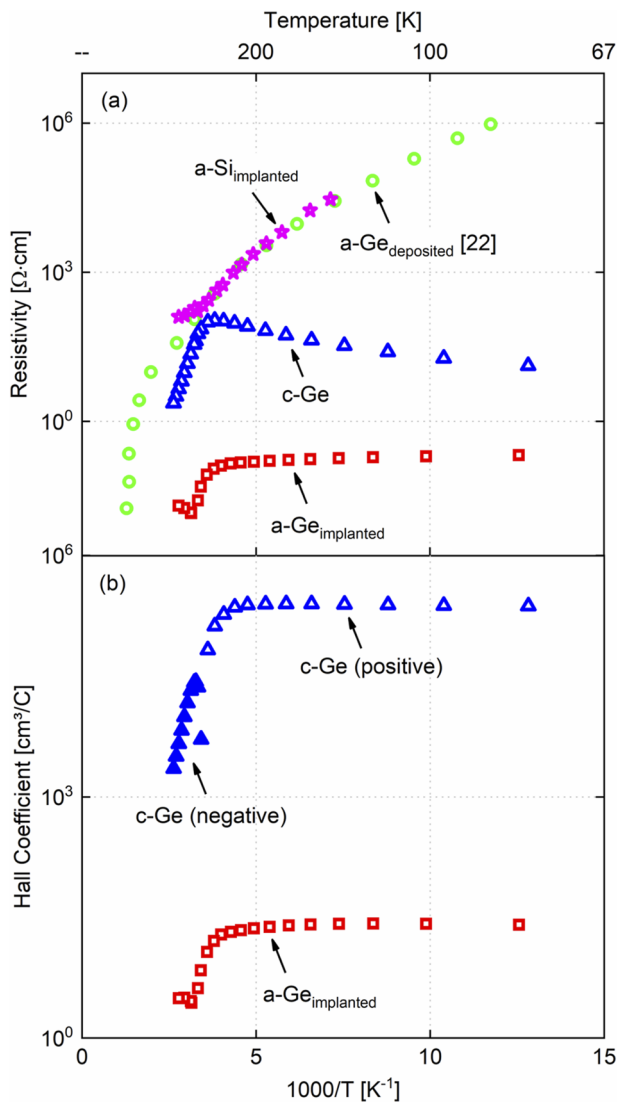
FIG. 4. Resistivity (a) and Hall coefficient (b) as a function of the reciprocal temperature ($1/T$) for c-Ge (blue-triangles), a-Ge by deposition (green-circles) from Ref. 28, a-Si by implantation (magenta-stars), and a-Ge by implantation (red-squares). For the Hall coefficient of c-Ge, R_H is positive (empty triangles) when $T < 275 K$. When $T > 275 K$, R_H is negative (filled triangle) but is presented as positive in (b) to be compatible with the logarithmic scale.

temperature range originates from extrinsic conductivity because of low levels of dopants (or impurities) in the starting materials. At a sufficiently high temperature (~275 K), thermal energy can excite electrons from the valence band into the conduction band, exponentially reducing the resistivity. This high-slope region is characterized by intrinsic conductivity involving band-to-band transitions in the materials. It is noticeable that the Hall coefficient of the c-Ge samples (blue-triangles) in Fig. 4(b) changes from positive in the extrinsic region to negative in the intrinsic region (but is plotted as positive to be compatible with the logarithmic scale). The sign of the Hall coefficient is indicated by empty (positive) and filled (negative) triangles. The change of conductivity from positive to negative can be explained by the fact that the conductivity of the c-Ge substrate is dominated by holes at low temperatures and then exhibits mixed-conductivity with both electrons and holes at higher temperatures. Because the Hall coefficient R_H for mixed conductivity depends on both electron and hole mobility, R_H becomes negative at the transition temperature due to the higher mobility of electrons. This carrier type-conversion phenomenon is well known and can be observed in lightly doped p-type c-Ge samples to occur at around room temperature.[27]

For the a-Ge samples, the difference between the measured resistivity of the implanted case (red-squares) and the thermally deposited one from Ref. 28 (green-circles) is substantial. For the deposited materials, the resistivity changes gradually without a sharp transition. In contrast, the resistivity curve of the implanted a-Ge is very well-defined and has a comparable behavior to that of c-Ge, with an extrinsic region for $T < 275 K$ (low T) and an intrinsic region for $T > 275 K$ (high T). The reason for the gradual change in resistivity of deposited a-Ge is that the band structure of the material is thought to be "fuzzy" due to localized band tails at the top of the valence band and the bottom of the conduction band.[28] In contrast, the band structure of our implanted a-Ge, based on the resistivity data, is clearly much more well-defined, closely resembling that of the crystal. At low temperatures, the resistivity of the implanted a-Ge is almost constant at around 0.1 Ωcm, which is 4–7 orders of magnitude lower than the typical values for deposited a-Ge. Furthermore, the conductivity of the implanted a-Ge in the extrinsic region ($T < 275 K$) is p-type as indicated by the positive Hall coefficient in Fig. 4(b). In other words, self-implanting Ge without any further treatment is likely to introduce a defect band very close to the valence band that behaves as acceptor levels. These defect levels, however, are not likely to alter the valence band significantly as shown by the temperature-dependent resistivity.

From the measured resistivity and the Hall coefficient data, we calculate the carrier mobility and the carrier density for the extrinsic conductivity region ($T < 275 K$). Note that we cannot easily examine the more complex intrinsic region ($T > 275 K$) because the mobility and carrier concentrations cannot be straightforwardly calculated for a mixed conductivity, at least without assumptions. In the extrinsic region, the conductivity is dominated by a single carrier type for both crystalline and implanted a-Ge because the resistivity of these two materials is almost constant with temperature. For a single carrier conductivity mechanism, the hole concentration, p, can be calculated from

$$p = \alpha \left(\frac{1}{R_H \cdot e} \right),$$

20 March 2024 08:52:23

where e is the elementary charge (1.6×10^{-19} C), α is a constant but, in general, can be ignored since it is always close to unity. In the worst case, α will introduce only a small error in the carrier concentration.[27] The carrier mobility can be found from

$$\mu = \frac{R_H}{\rho}.$$

The deduced data for the carrier concentration p and the carrier mobility μ of c-Ge and a-Ge are shown in Fig. 5. The carrier density of the implanted a-Ge (magenta-diamonds) is of the order of 10^{17} cm^{-3} and is p-type. The carrier concentration remains largely constant within the temperature range, which means that most acceptor levels are very close to the valence band edge and are fully ionized with very low thermal energy. Tauc et al. have estimated the activation energy of these acceptors as $E_A \geq 0.01$ eV.[10]

Treating c-Ge first, the mobility of c-Ge (blue-triangles) in Fig. 5 is in excellent agreement with studies by Morin and Maita.[30] In general, carrier mobility depends on impurity and lattice scattering. However, impurity scattering in high quality materials decreases as the temperature increases and is negligible for $T > 100$ K. Due to acoustic lattice scattering, the carrier mobility should exhibit a temperature dependence given by $\mu_{ac} = AT^{-1.5}$. From Morin's study, experimental data of c-Ge in the range of 100–300 K showed a temperature dependence of $T^{-1.66}$ for electrons and $T^{-2.33}$ for holes, deviating from the $T^{-1.5}$ law.[30] Our experimental data in Fig. 5 exhibit a dependence of $T^{-2.35}$ for holes, which closely matches Morin's value.

For the a-Ge case, the carrier mobility of the deposited material is in the order of 10^{-3} cm^2/(Vs) (green-circles), typical of values found in the literature for deposited a-Ge.[29] According to a theoretical calculation, one would expect the Hall mobility in the variable-range-hopping regime to be around 10^{-4} cm^2/(Vs).[31]
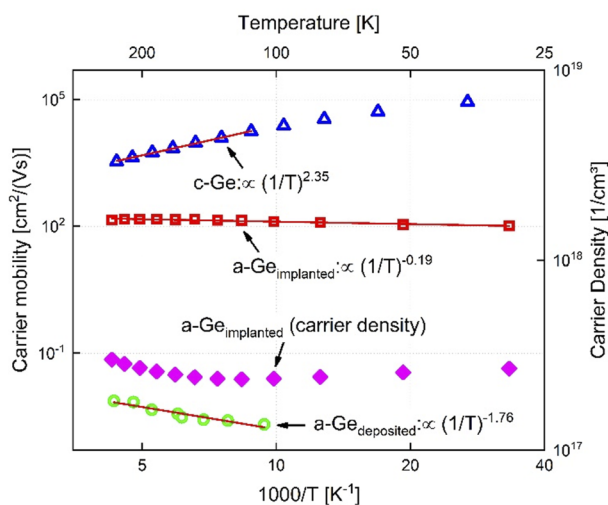
Remarkably, the mobility of a-Ge produced by implantation is found to be exceptionally high, in the order of 10^2 cm^2/(Vs) (red-squares). At this moment, it is worth re-visiting the optical study by Tauc et al. who reported a number of findings on the band structure of deposited a-Ge.[9–11] The absorption spectra at photon energies of 0.08–0.6 eV showed several direct transitions between the three branches of the valence band, similar to what is observed in p-type c-Ge. These absorption spectra of the a-Ge can be well described by the same set of formulas used for Ge crystals, whereby the effective masses of heavy holes m_1, light holes m_2, and the energy gap of the spin–orbit splitting ΔE are comparable to those for crystalline Ge. Hence, it is suggested that the valence band is essentially preserved in a-Ge, and the wave function can be described by Bloch functions for non-localized waves. Based on previous electrical data for deposited a-Ge, this proposal by Tauc et al. was not accepted by others.[8,28,32,33] However, consistent with Tauc's findings, our measurements for implanted a-Ge show a very well-defined behavior of the resistivity with temperature (Fig. 4), and the carrier mobility is extremely high for an amorphous semiconductor, in the order of 10^2 cm^2/(Vs) (Fig. 5). These results provide direct evidence for non-localized states of the valence band in a-Ge as suggested by Tauc et al. Also, it is worth noting that our measurement of implanted a-Si showed a resistivity of 10^2–10^4 Ωcm (Fig. 4(a)/magenta-stars), which is 4–6 orders of magnitude higher than that of the implanted a-Ge, indicating a fundamental difference in the conductivity mechanism between a-Si and a-Ge. While a-Si can be characterized by hopping conduction, carrier transport in pure ion implanted a-Ge is very likely to be non-localized.

To account for the large difference in electrical results measured in implanted a-Ge and the previous data for deposited a-Ge, we propose that it is not due to the intrinsic nature of a-Ge but mostly dictated by mass-density fluctuations and impurities within the deposited materials. This scenario was previously adopted by Stuke for amorphous selenium[34] and later adopted by Tauc for a-Ge.[11] The density fluctuations in these materials may cause different types and concentrations of defects, such as dangling bonds, different bonding configurations, and internal strain, all of which can create potential barriers to carrier transport. Tauc speculated that a potential barrier of ~0.1 eV would be sufficient for the 4 orders of magnitude difference between the conductivity of deposited a-Ge and that expected if extended electron wave functions were dominant.[11]

The near-crystalline mass density and material uniformity are not the only reasons for the high carrier mobility in implanted a-Ge. The a-Ge material also has substantially higher carrier mobility than implanted a-Si as mentioned above, despite that the valence band structure of c-Si and c-Ge are quite similar, and it could be argued that a-Si should also have these non-localized states and corresponding high mobility. However, one reason why a-Si does not have high mobility could be that Ge is more effective in minimizing unsaturated dangling bonds and vacancies during the implantation, or that such dangling bonds in a-Ge do not lead to defect-induced de-localization. Indeed, it is well-known that implanted Ge develops into a porous structure because of defect mobility during implantation, and this behavior may lead to fewer dangling bonds and defect states, whereas implanted Si does not exhibit such behavior under any implantation conditions.[17,35] We thus believe that the different behaviors of the two materials during ion implantation are
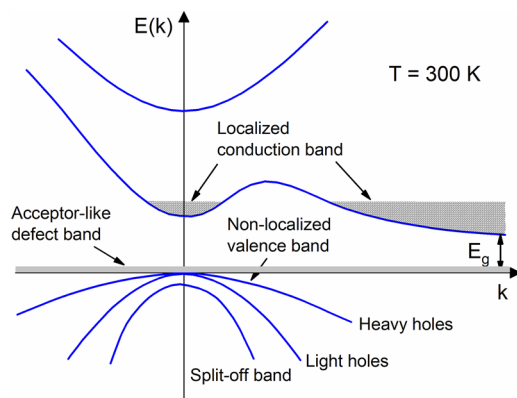

FIG. 5. Carrier mobility as a function of reciprocal temperature ($1/T$) for c-Ge (blue-triangles), a-Ge by deposition (green-circles),[29] and a-Ge by implantation (red-squares). Magenta-diamond is the carrier density of the a-Ge by implantation (right hand scale).

FIG. 6. A simplified band structure of amorphous germanium according to the results of this study and available Refs. 9–11. The solid curves represent the conduction band and the valence band of crystalline Ge. The darker regions represent the localized states in the conduction band and the accepter-like defect level close to the valence band in a-Ge.

one of the reasons for the contrasting electrical properties of these as-implanted amorphous materials.

Based on the results of this study and understanding from the existing literature, we plot a simplified band structure of amorphous Ge as shown in Fig. 6. The structure is featured a narrow acceptor-like defect band very close to the valence band. The shape and position of this defect band very close to the valence band give rise to a very low thermal activation energy of the carriers. This results in the almost constant carrier density shown in Fig. 5 as a function of temperature. The top of the valence band is preserved or almost preserved (that is, consists of non-localized states) as shown by the very high hole mobility measured in this study and also the optical results in Ref. 10. In contrast, the states at the bottom of the conduction band are likely to be localized, as suggested by Tauc's optical data. For our electrical data of a-Ge, there is no conduction type switching from positive to negative [Fig. 4(b), red square] as found in c-Ge. This might also suggest the localization of the conduction band states in a-Ge so that the electron mobility is not sufficient for the change of sign in the Hall coefficient.

For practical applications, first, the high-mobility a-Ge can be used for high performance flexible and transparent electronics. Second, as Dohler and Brodsky suggested, the type of amorphous–crystalline heterojunctions is helpful for reducing the Fermi level pinning (FLP) effect in the conventional Schottky metal–semiconductor junction.[36,37] The FLP effect is believed due to surface states and strong interface polarization, which are both absent in the amorphous–crystalline interface. The FLP effect is known to be particularly strong in metal-Ge junctions. Adding the thin amorphous interlayer would reduce this effect. To some extent, this solution has been demonstrated by Lieten *et al.*[38]

CONCLUSIONS

We have shown data for the electrical characterization of amorphous Ge prepared by a conventional ion beam amorphization. The material prepared by this method is pure, with a mass-density close

to that of crystalline Ge, and fully amorphous as indicated from pre-implant simulation studies and shown by selective area electron diffraction. Such ion implanted a-Ge can be considered a model system since the sample-to-sample variation in mass density and impurity content is avoided. Therefore, electrical transport that was solely related to the amorphous nature of the material could be studied. We have found that the hole mobility of the material is extremely high, in the order of $\sim 10^2 \, \mathrm{cm^2/(Vs)}$, which is 4–6 orders of magnitude higher than conventional a-Ge prepared by deposition techniques. This is also one of the highest mobilities in all types of amorphous semiconductors. We ascribed this property to the preservation of non-localized states in the valence band of a-Ge. Furthermore, the defect levels introduced by the self-implantation are acceptor-like and very close to the valence band, which produced a hole concentration of $10^{17} \, \mathrm{cm^{-3}}$. Overall, our findings are suggested to provide a pathway to substantially improve the properties of a-Ge for low cost, high performance thin film devices.

SUPPLEMENTARY MATERIAL

In the supplementary material, we provide data for the irradiation simulation using SRIM, the XRD result of the sample before and after irradiation, and the SAED/TEM result of different regions of the sample.

AUTHOR DECLARATIONS

Conflict of Interest

The authors have no conflicts to disclose.

AUTHOR CONTRIBUTIONS

T.T. and J.W. conceptualized the research. T.T. and J.W. conducted and analyzed the Hall effect measurement. T.T. and L.S. conducted and analyzed the TEM data. All authors discussed the results and commented on the manuscript. T.T. wrote the final manuscript. The manuscript was written through contributions of all authors. All authors have given approval to the final version of the manuscript.

Tuan T. Tran: Conceptualization (lead); Data curation (lead); Formal analysis (lead); Investigation (lead); Methodology (lead); Writing – original draft (lead); Writing – review & editing (lead). **Jennifer Wong-Leung**: Data curation (supporting); Formal analysis (supporting); Methodology (supporting); Writing – review & editing (supporting). **Lachlan A. Smillie**: Data curation (supporting); Visualization (supporting). **Anders Hallén**: Data curation (supporting); Formal analysis (supporting); Writing – review & editing (supporting). **Maria G. Grimaldi**: Conceptualization (supporting); Funding acquisition (supporting); Writing – review & editing (supporting). **Jim S. Williams**: Conceptualization (equal); Data curation (supporting); Formal analysis (supporting); Funding acquisition (lead); Methodology (equal); Project administration (lead); Resources (lead); Supervision (lead); Writing – original draft (equal); Writing – review & editing (equal).

DATA AVAILABILITY

The data that support the findings of this study are available from the corresponding author upon reasonable request.

REFERENCES

[1] A. Madan and M. P. Shaw, *The Physics and Applications of Amorphous Semiconductors* (Elsevier, 2012).

[2] A. H. Clark, J. Non-Cryst. Solids **2**, 52 (1970).

[3] A. I. Gubanov, *Quantum Electron Theory of Amorphous Conductors* (Springer Science & Business Media, 2012).

[4] E. A. Davis and N. F. Mott, Philos. Mag. **22**, 0903 (1970).

[5] R. A. Street, *Hydrogenated Amorphous Silicon* (Cambridge University Press, 2005).

[6] W. Beyer and J. Stuke, Phys. Status Solidi A **30**, 511 (1975).

[7] P. A. Walley and A. K. Jonscher, Thin Solid Films **1**, 367 (1968).

[8] A. H. Clark, Phys. Rev. **154**, 750 (1967).

[9] J. Tauc, Science **158**, 1543 (1967).

[10] J. Tauc, R. Grigorovici, and A. Vancu, Phys. Status Solidi B **15**, 627 (1966).

[11] J. Tauc, Mater. Res. Bull. **3**, 37 (1968).

[12] T. M. Donovan, W. E. Spicer, J. M. Bennett, and E. J. Ashley, Phys. Rev. B **2**, 397 (1970).

[13] T. B. Light, Phys. Rev. Lett. **22**, 999 (1969).

[14] G. Impellizzeri, S. Mirabella, and M. G. Grimaldi, Appl. Phys. A **103**, 323 (2011).

[15] L. Romano, G. Impellizzeri, and M. G. Grimaldi, Mater. Sci. Semicond. Process. **15**, 703 (2012).

[16] K. Laaziri, S. Roorda, and J. M. Baribeau, J. Non-Cryst. Solids **191**, 193 (1995).

[17] T. T. Tran, H. S. Alkhaldi, H. H. Gandhi, D. Pastor, L. Q. Huston, J. Wong-Leung, M. J. Aziz, and J. S. Williams, Appl. Phys. Lett. **109**, 082106 (2016).

[18] H. S. Alkhaldi, T. T. Tran, F. Kremer, and J. S. Williams, J. Appl. Phys. **120**, 215706 (2016).

[19] J. F. Ziegler, M. D. Ziegler, and J. P. Biersack, Nucl. Instrum. Methods Phys. Res., Sect. B **268**, 1818 (2010).

[20] Y. Shacham-Diamand, A. Sinar, E. R. Sirkin, I. A. Blech, and L. Gerzberg, IEEE Trans. Electron Devices **37**, 159 (1990).

[21] D. T. Tran, G. Svensson, and C.-W. Tai, J. Appl. Crystallogr. **50**, 304 (2017).

[22] G. Etherington, A. C. Wright, J. T. Wenzel, J. C. Dore, J. H. Clarke, and R. N. Sinclair, J. Non-Cryst. Solids **48**, 265 (1982).

[23] C. J. Benmore, R. T. Hart, Q. Mei, D. L. Price, J. Yarger, C. A. Tulk, and D. D. Klug, Phys. Rev. B **72**, 132201 (2005).

[24] S. Dalgiç, L. E. Gonzalez, S. Baer, and M. Silbert, Physica B **324**, 292 (2002).

[25] F. Alvarez, C. C. Díaz, A. A. Valladares, and R. M. Valladares, Phys. Rev. B **65**, 113108 (2002).

[26] H. Richter and O. Fürst, Z. Naturforsch. A **6**, 38 (1951).

[27] E. H. Putley, *The Hall Effect and Related Phenomena* (Butterworths, 1960).

[28] K. L. Chopra and S. K. Bahl, Phys. Rev. B **1**, 2545 (1970).

[29] R. A. Lomas, M. J. Hampshire, R. D. Tomlinson, and K. F. Knott, Phys. Status Solidi A **16**, 385 (1973).

[30] F. J. Morin and J. P. Maita, Phys. Rev. **94**, 1525 (1954).

[31] L. Friedman and M. Pollak, Philos. Mag. B **44**, 487 (1981).

[32] M. Morgan and P. A. Walley, Philos. Mag. **23**, 661 (1971).

[33] M. Pollak, M. L. Knotek, H. Kurtzman, and H. Glick, Phys. Rev. Lett. **30**, 856 (1973).

[34] J. Stuke, Phys. Status Solidi B **6**, 441 (1964).

[35] B. R. Appleton, O. W. Holland, J. Narayan, O. E. Schow III, J. S. Williams, K. T. Short, and E. Lawson, Appl. Phys. Lett. **41**, 711 (1982).

[36] G. H. Doőhler and M. H. Brodsky, AIP Conf. Proc. **20**, 351 (1974).

[37] M. H. Brodsky and G. H. Dohler, CRC Crit. Rev. Solid State Sci. **5**, 591 (1975).

[38] R. R. Lieten, S. Degroote, M. Kuijk, and G. Borghs, Appl. Phys. Lett. **92**, 022106 (2008).